Am J Cancer Res 2017;7(9):1804-1819
www.ajcr.us /ISSN:2156-6976/ajcr0060210

Original Article

Zinc finger RNA-binding protein promotes non-small-cell carcinoma growth and tumor metastasis by targeting the Notch signaling pathway

Heng Zhang, Chun Fang Zhang, Ri Chen

Department of Cardiothoracic Surgery, Xiangya Hospital of Central South University, 87# Xiangya Road, Changsha 410008, Hunan, China

Received June 25, 2017; Accepted July 10, 2017; Epub September 1, 2017; Published September 15, 2017

Abstract: Metastatic non-small-cell lung carcinoma (NSCLC) is typically incurable. The development of anti-metastatic therapies is hampered because the mechanisms regulating metastasis in NSCLC are not well known. Currently, there is no effective treatment for NSCLC once it has progressed to the metastatic stage. Therefore, further elucidation of the molecular mechanisms underlying the metastasis of NSCLC cells is urgently required for improving NSCLC treatment. Here, we report that the zinc finger RNA-binding protein (ZFR) is over-expressed in NSCLC cells and demonstrate that ZFR is a promising therapeutic target in metastatic NSCLC. The use of shRNA to knockdown ZFR impaired cell proliferation *in vitro* and tumor growth *in vivo*. Moreover, silencing of ZFR inhibited metastasis almost completely. In contrast, over-expression of ZFR in cells significantly enhanced NSCLC cell growth and metastasis. Finally, ZFR increased the metastatic potential of NSCLC cells in a Notch1-dependent manner. Collectively, our study reveals a critical role of ZFR in NSCLC tumor growth and metastasis, suggesting ZFR as a novel target for the treatment of NSCLC.

Keywords: NSCLC, ZFR, Notch1, metastasis

Introduction

Non-small-cell lung carcinoma (NSCLC) is the deadliest lung cancer and has a steadily increasing incidence rate [1]. NSCLCs account for about 85-90% of lung cancer cases, which encompass lung adenocarcinomas, lung squamous cell carcinomas, and large cell carcinomas [2]. Tumorigenesis of NSCLC is induced by acquired driver mutations, for example, in the Neuroblastoma RAS Viral Oncogene Homolog (NRAS) or B-Raf Proto-Oncogene (BRAF) loci [3]. Moreover, genes known to regulate metastasis of NSCLC cells have been associated with the prognosis of patients with NSCLC [4]. NSCLC aggressiveness is based on the highly metastatic potential of cancer cells, but these cells still cannot be efficiently targeted despite recent progresses in NSCLC therapies [5]. Tumor metastasis to regional lymph nodes, as detected by analysis of sentinel lymph nodes, frequently represents the first step of NSCLC dissemination and serves as an important prognostic indicator. Metastasis is considered critical for the migration of tumor cells from an initial location to another soft tissue [6]. This was proven to be one of the trademarks of cancer and is the real risk factor of NSCLC. Thus, identification of new therapeutic targets for metastatic NSCLC is crucial.

In order to identify genes involved in the metastasis of NSCLC cells, we transfected H1975 human NSCLC cells with a specifically designed retroviral vector, pDisrup 8, which randomly disrupts genes in the genome. The vector-bearing cell clones were selected using blasticidin and then screened by a wound healing assay to determine their migration potential. Cell clones with increased or decreased migratory potential were subjected to 3' RACE to identify genes involved in the metastasis of NSCLC cells [7]. As a result, we found that the zinc finger RNA-binding protein (ZFR) is involved in the metastasis of NSCLC. Zinc finger proteins, encoded by zinc finger RNA-binding (ZFR) gene, were reported to play an important role in DNA-binding and regulation of growth and development. ZFR is

an ancient chromosome-associated protein that is highly conserved from nematodes to mammals. The murine ZFR protein was identified in a screen for RNA-binding proteins expressed during spermatogenesis. The human ZFR appears to be involved in the regulation of alternative pre-mRNA splicing and was identified in a screen for factors that interact with the pre-mRNA splicing activator RNPS1 [8]. Transcript levels of ZFR were determined in various human tissues but were undetectable in skeletal muscle. The knockdown of ZFR by RNA interference in neurons relocated the Staufen 2 (62) isoform to the nucleus, which suggests that ZFR is critical for Staufen 2 isoform-specific nucleocytoplasmic shuttling in neurons and likely has key functions during the early steps of RNA transport and localization [9]. TDP-43 was shown to be a major disease-associated protein in most cases of amyotrophic lateral sclerosis (ALS), tau-negative frontotemporal lobar degeneration (FTLD), and inclusion body myopathy. Mass spectrometry identified ZFR as one of the TDP-43-interacting proteins. In addition, ZFR was demonstrated to direct the targeted chromosomal integration of a plasmid at specific recognition sites, distributed throughout human genomes, in several cell types. Despite recent obtained advances in understanding the biological functions of ZFR, little is known about the effects of ZFR on NSCLC diagnosis and prognosis.

In the present study, we demonstrated using insertional mutagenesis, that ZFR is involved in the metastasis of H1975 NSCLC cells. We demonstrated that ZFR disruption impairs metastasis of H1975 cells. The requirement of ZFR for the migration of NSCLC cells was further confirmed by gene silencing using shRNA in vitro. In line with this result, over-expression of ZFR significantly promoted the migratory ability of H1975 cells. Moreover, down-regulation of ZFR expression in H1975 cells strikingly inhibited their cellular metastasis in vivo. ZFR inhibition in H1975 cells by shRNA suppressed tumor growth in nude mice. Conversely, NSCLC-specific ZFR over-expression enhanced tumorigenicity and growth of NSCLC cells in vivo. Finally, we found that ZFR promoted H1975 cell migration and invasion via the Notch1 signaling pathway. In conclusion, our findings suggest a novel mechanism underlying the metastasis of NSCLC that may serve as a new intervention target for the treatment of NSCLC.

Materials and methods

Cell culture and patients specimens

NSCLC H1975, A549, HCC827, H1299, H1650 and normal lung cell line LO2 were obtained from the Chinese Academy of Sciences Cell Bank of Type Culture Collection (CBTCCCAS, Shanghai, China). The cancer cell lines were cultured as monolayers in RPMI 1640 culture media or DMEM supplemented with 10% fetal bovine serum (Wisent, Quebec, Canada), 100 μg/mL penicillin, and 100 μg/mL streptomycin maintained in an incubator with a humidified atmosphere of 95% air and 5% CO_2 at 37°C. Specific inhibitor for Notch (FLI-06) was obtained from Selleck (USA). Lipofectamine 2000 was purchased from Invitrogen (USA). 18 tumor tissues which, were used for immunohistochemical analysis, were obtained from the Alenabio (BC04021, Xian, China). All tissues were collected immediately upon resection of the tumors in the operation theater, transported in liquid nitrogen, and then stored at -80°C. Tumor staging was based on the 6th edition of the tumor-node-metastasis (TNM) classification of the International Union against Cancer. This study was approved by the Research Ethics Committee of Xiangya Hospital of Centre-south University.

MTT assays

The cell viability was determined by CellTiter 96® AQueous One Solution cell proliferation assay (Promega, Madison, WI, USA). Briefly, cells were seeded in 96-well cell culture plates. After incubation for indicated time period, 20 μL of One Solution reagent were added to each well and incubation was continued for additional 4 h. The absorbance was measured at 490 nm using Synergy™ HT Multi-Mode Microplate Reader (Bio-Tek, Winooski, VT, USA) [10].

Plasmids and DNA constructs

The pDisrup retroviral vector was constructed based upon MMLV retroviral vector pLNCX as backbone. The splicing donor and acceptor were designed according to human adenovirus type 2 major late mRNA intron sequence. For pDisrup clone selections, cells were selected with Blasticidin S. HCl at 25 μg/ml (Invitrogen, USA). The short small interfering RNA (shRNA) was constructed with sequence specifically targeted to ZFR was obtained from Santa Cruz

(Santa Cruz Biotechnology, USA). The Myc-tagged pCLEN-Notch1 (Plasmids # 17704, Addgene, Cambridge, MA) was deposited by Dr. Nicholas Gaiano. Oligonucleotides for human Notch1 siRNA kit were purchased from OriGene (Rockville, MD, USA). The kit contains three predesigned duplexes targeting a specific gene of interest, and we used a pool of three target siRNAs to ensure work efficiency. Transient transfection was performed using the Lipofectamine RNAi MAX reagent (Invitrogen) and following the manufacturer's instructions.

Oncomine analysis

The expression level of ZFR genes in the NSCLC was analyzed using Oncomine. For this, we compared clinical specimens of cancer vs. normal patient from the in Weiss Lung database and Hou Lung database. In order to reduce our false discovery rate, we selected $P < 0.01$ as a threshold. We analyzed the results for their *p*-values and fold change.

Western blot

After washing with PBS (3.2 mM Na_2HPO_4, 0.5 mM KH_2PO_4, 1.3 mM KCl and 140 mM NaCl, pH 7.4) twice, cells were extracted with cold lysis buffer (20 mM Tris, 100 mM NaCl, 5 mM EDTA, 1 mM EGTA, 5 mM $MgCl_2$, 1% Triton X-100, 2.5 mM sodium pyrophosphate, 1 mM b-glycerolphosphate, 1 mM Na_3VO_4, 1 mM PMSF, and Roche complete protease inhibitors) and centrifuged at 15,000 g for 15 min at 4°C. Protein concentration of the supernatants was determined with Bradford assay (Biorad, USA). 30 μg of samples was separated by electrophoresis on 10% SDS-PAGE and transferred to Polyvinylidene fluoride membrane (Millipore, USA). After blocking with 5% skimmed milk for 1 h, membranes were incubated with different specific primary antibodies in either 5% skimmed milk or 5% bovine serum albumin (BSA) (anti-ZFR, anti-Ntoch1, anti-PI3K phospho-PI-3K, AKT, phospho-AKT, mTOR, phospho-mTOR, p70 S6, phospho-p70 S6 from Cell Signaling Technology) [11]. After washing with PBST for 30 min, the membranes were further incubated with corresponding HRP-conjugated secondary antibodies and developed with Pierce's West Pico chemiluminescence substrate (Millipore, USA). All results were obtained from 3 independent experiments.

Wound healing assay

Wound healing assay was performed as previously described. Briefly, H1975 cells were seeded in 60 mm dishes and cultured at 37°C overnight to produce a confluent monolayer. After starvation in serum-free medium for 24 hours, a wound was created by scratching the monolayer with a 200 μl yellow sterile pipette tip. The wounded monolayer was then washed twice to remove cell debris and incubated with fresh normal medium. The area of cell-free scratch was photographed at 0 h and 24 h after scratching respectively. The wound healing effect was determined by measuring the percentage of the remaining cell-free area compared with the area of the initial wound [12].

Colony formation assay

Cells were seeded in triplicate at 500 cells/6-cm dish in complete medium. After 3 weeks of growth, cells were fixed and stained with 0.1% crystal violet, and visible colonies were counted according to the number of cells in each colony. All experiments were repeated at least three times. Plating efficiency was determined as the number of colonies formed divided by the total number of cells plated [13].

In vitro invasion assay

Invasion of NSCLC cells was determined by BD BioCoat™ Matrigel™ Invasion Chamber (BD Biosciences, USA) assay in vitro according to the manufacturer's instructions. In brief, 1×10^5 cells with 500 μl in serum-free medium were added into the upper chamber and 750 μl 1640-medium was added into the lower chamber, serving as chemo-attractant. After incubation in humidified tissue culture incubator, 37°C, 5% CO_2 atmosphere for 24 h, the non-invasive cells in the upper surface of the membrane were removed by "scrubbing" with cotton tipped swab and the invasive cells migrating to the lower surface of the membrane were fixed and stained with 0.1% crystal violet for 30 minutes. Cell counting was then carried out by photographing the membrane through the microscope. 5 random fields under microscope at 20X magnification are taken [14].

Immunocytochemistry

After cells on glass coverslips were treated by indicated agents, they were fixed by pre-cold

acetone, then rinsed three times with PBS. The cells were permeabilized in 0.1% Triton X-100 and incubated with 1% BSA/PBS to block non-specific binding. Subsequently, the cells were immunostained by incubating with rabbit monoclonal antibody against ZFR (diluted 1:500, Epitomics) overnight at 4°C. After being washed with PBS, cells were incubated with FITC-conjugated goat anti-rabbit secondary antibody (diluted 1:60, Boster Biotechnology, Wuhan, China). Nuclei were counterstained with DAPI (Biotime Biotech, Haimen, China). Images were taken and analyzed using the ZEN 2011 imaging software on a Zeiss invert microscope (CarlZeiss, Hallbergnoos, Germany) under 400-fold magnification [15].

Experimental metastasis assay

Female C57BL/6J mice at 6-8 weeks old (15-20 g) were purchased from the laboratory Shanghai Slack Laboratory Animal Co., LTD. Mice were maintained at dark/light cycles of 12 h duration with food and water available ad libitum. 24 animals were randomly divided into four experiment groups. For experimental metastasis analysis, the mice were injected at the lateral tail vein with (5×10^5) B16F10 cells carrying control, ZFR OE, or ZFR shRNA plasmids. Mice were sacrificed 2 weeks after inoculation and all organs were examined for the presence of macroscopic metastases. Lung and liver metastatic nodules were determined under a dissecting microscope [16]. Animal handling and experimental procedures were approved by the Institutional Animal Care and Use Committee (IACUC) of Xiangya Hospital of Centre-south University.

Quantitative real-time PCR

Total RNA was extracted using the RNEasy kit (Qiagen). Reverse transcription reactions were performed on 1 μg of RNA with the QuantiTect Reverse Transcription kit (Qiagen). The primers used for PCR were as follows (sense and antisense, respectively): GAPDH: Forward: 5'-CTCACCGGATGCACCAATGTT-3', Reverse: 5'-CGCGTTGCTCACAATGTTCAT-3'; Notch1: Forward: 5'-GAGGCGTGGCAGACTATGC-3', Reverse: 5'-CTTGTACTCCGTCAGCGTGA-3'. PCR amplifications were performed with the MESA GREEN qPCR MasterMix (Eurogentec) on an ABI Prism 7500 thermal cycler. The gene screening was conducted with the RT2 Profiler PCR EMT Array (Qiagen).

Xenograft models and immunohistochemistry detections

3×10^6 H1975 cells were subcutaneously implanted into female, BALB/c nude mice to build NSCLC xenograft. On the seventh day, mice with appropriate size (150-300 mm^3) of tumors were divided randomly into five groups. Tumor volume and mice body weight were measured every 3 days. Tumor volume was calculated as $mm^3 = 0.5 \times \text{length (mm)} \times \text{width (mm)}^2$. After sacrificing mice on day 21, deparaffinized tumor sections were stained with specific antibody for ZFR. Detection was done with avidin-biotin-HRP complex (Thermo scientific) and diaminobenzidine as chromogen. Nuclei were counterstained with hematoxylin [17]. Animal handling and experimental procedures were approved by the Institutional Animal Care and Use Committee (IACUC) of Xiangya Hospital of Centre-south University.

Statistical analysis

The data were presented as mean ± SD. Differences in the results of two groups were evaluated using either two-tailed Student's t test or one-way ANOVA followed by post hoc Dunnett's test. The differences with $P < 0.05$ were considered statistically significant.

Results

ZFR is a novel regulator of NSCLC metastasis

The tumor cell line H1975 is a commonly utilized model system to determine the movement and invasion of NSCLC due to its highly metastatic potential. To identify vital genes participating in the movement and invasiveness of NSCLC cells, the pDisrup vector was transfected into H1975 cells; this vector unsystematically integrates into the genomic DNA and contains a blasticidin resistance gene that allows selection of H1975 cells containing the mutated genes. The migration potential of the selected mutant H1975 clones was verified by the Transwell assay. Subsequently, clones exhibiting higher or lower migration ability compared to controls were further analyzed by RT-PCR and 3' RACE to identify genes that were mutated by the pDisrup vector. Many prospective genes were detected, including ZFR. The clone exhibiting a lowered movement capacity was named ZFR^{mut}. To determine whether ZFR was actually mutated in the H1975 NSCLC cells, both Western Blot and cell immunofluores-

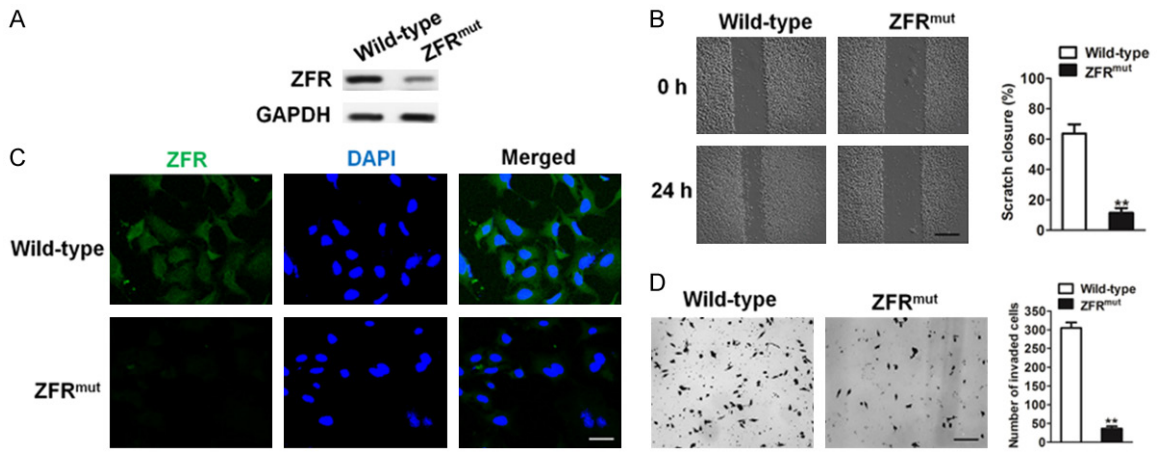

Figure 1. Identification of a novel role of ZFR in the metastasis of NSCLC cells. A. ZFR^{mut} cells and wild type H1975 cell were subjected to western blot for measuring protein level of ZFR. B. Cells were fixed and incubated with primary antibodies against ZFR and then were immunostained with anti-rabbit FITC-conjugated secondary antibody and then stained with DAPI. The specimens were visualized and photographed using a fluorescence microscope. Scale bar represents 50 μm. C. Wound healing assay of wild-type cells and ZFR^{mut} cells was performed. The amount of cell movement was calculated. The data shown were represented as the mean ± SD. For indicated comparison, $^{**}P < 0.01$ compared to wild type cells. Scale bar represents 200 μm. D. The cell invasion potency was evaluated by Transwell invasion assay. Representative picture was generated post staining with crystal violet. The data shown were represented as the mean ± SD. For indicated comparison, $^{**}P < 0.01$ compared to wild type cells. Scale bar represents 100 μm.

cence assays were performed. As indicated in **Figure 1A** and **1B**, ZFR protein expression was considerably inhibited in ZFR^{mut} cells compared to that in the control cells. Quantitative real-time polymerase chain reaction (qRT-PCR) analysis demonstrated that ZFR was expressed in wild-type cells but not in ZFR^{mut} H1975 cells (Supplementary Figure 1). To examine the function of ZFR in H1975 metastasis, we conducted a wound healing analysis and a Transwell invasion assay to assess cell mobility. As described in **Figure 1C**, control cells fully recovered the scratched area within 24 h; however, the ZFR^{mut} cells were 20% slower and unable to close the wound before the endpoint. Consistently, compared to the wild-type cells, fewer ZFR^{mut} cells migrated across the Matrigel membrane of the Transwell (**Figure 1D**). In short, interruption by ZFR protein inhibition reduces H1975 cancer cell migration and invasion in vitro.

ZFR is over-expressed in NSCLC

To investigate whether ZFR is involved in tumor progression, we first extracted data of transcript expression for ZFR from the publicly accessible Oncomine microarray database for lung. In two independent clinical data sets containing ZFR information, ZFR expression was markedly increased in neoplastic skin tissues compared to that in normal skin tissues (**Figure 2A**). The correlation between ZFR levels and the clinical outcomes of a NSCLC patient was further examined using the online biomarker validation tool, KM-plotter (http://kmplot.com/analysis). This platform derives risk groups and Kaplan-Meier curves with different expression levels. Statistical analysis (**Figure 2B**) revealed that up-regulation of ZFR correlated with a decreased overall survival (P = 0.0027). Immunohistochemical labeling of ZFR in clinical NSCLC biopsies (n = 18) further confirmed ZFR protein expression in NSCLC cells (**Figure 2C**). The association between cancer progression and increased expression was also confirmed in a panel of cell lines. ZFR was expressed in relatively high levels in the invasive cell lines H1975, A549, HCC827, H1299 and H1650, but was markedly reduced in untransformed human lung cells LO2 (**Figure 2D**). This ZFR overexpression was partially due to an increase in ZFR mRNA levels, as shown by qRT-PCR (**Figure 2E**). Together with the results of the systemic analysis, these results suggest that overexpression of ZFR is a prognostic biomarker for poor survival rate in NSCLC.

Endogenous ZFR regulates NSCLC cell metastasis

To confirm that ZFR down-regulation is responsible for the declined metastasis of NSCLC ce-

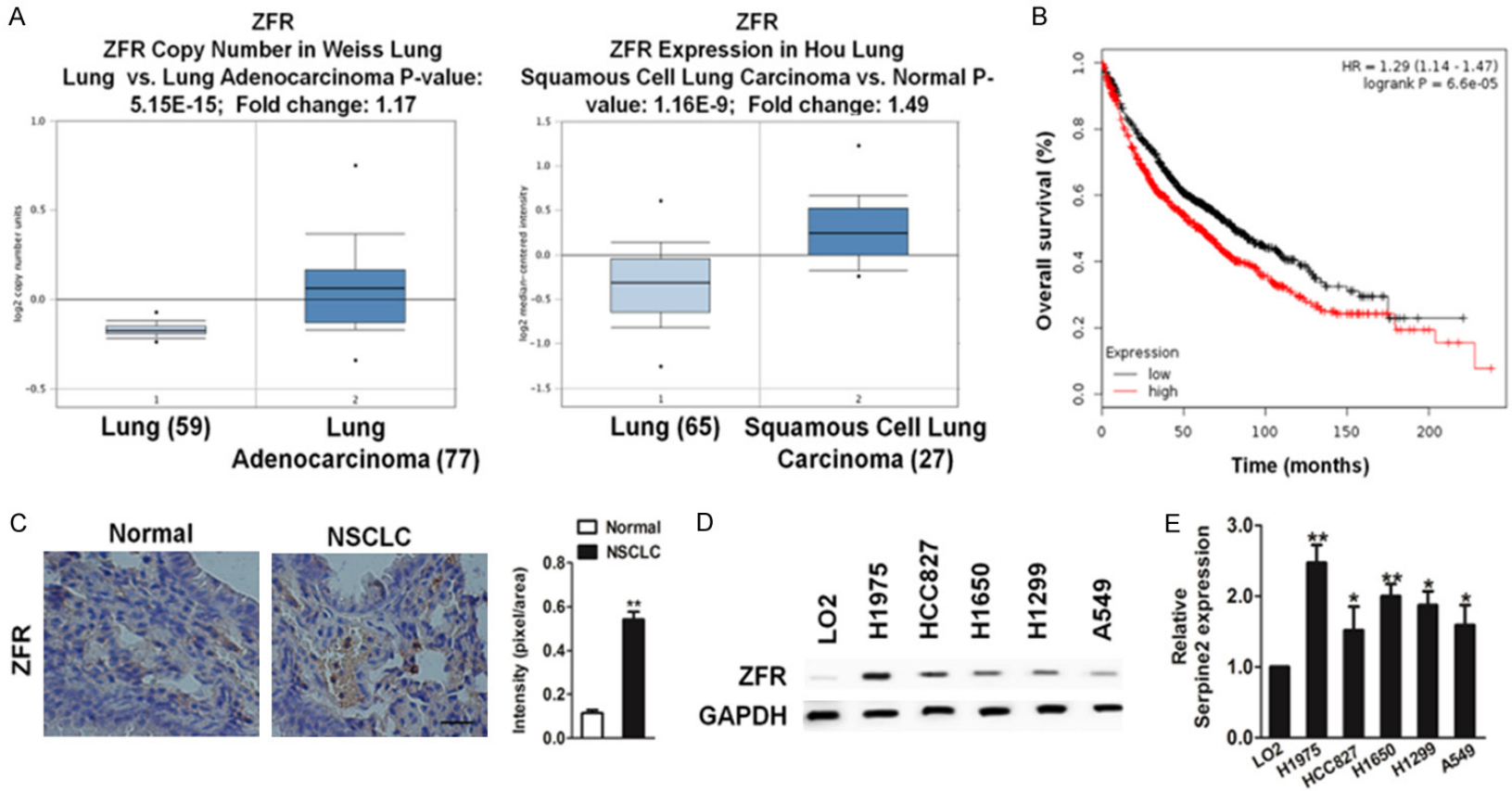

Figure 2. ZFR is over-expression in NSCLC. A. Box plots show increased levels of ZFR in NSCLC (right) compared with normal skin tissues (left) in two microarray data sets. $^{**}P < 0.01$ compared with normal lung tissues. B. Expression level of ZFR was associated to prognosis in patients with NSCLC. Kaplan-Meier survival curve showing the survival of NSCLC patients with high or low ZFR expression. High and low expressions were represented in red and black, respectively. C. Immunohistochemical staining of ZFR in I human NSCLC tissue (n = 18) and normal tissues (n = 18). The intensity of ZFR staining was quantified using ImageJ Plus and shown in the box plot below. Scale bars represent 50 μm. $^{**}P < 0.01$, compared with normal skin tissues. Scale bar represents 50 μm. D. Immunoblotting analysis of ZFR protein in the NSCLC cell resections and human normal lung cells LO2. ZFR protein expressions were up-regulated in all NSCLC cell lines examined compared with that in LO2. E. Total RNAs were extracted from a series of NSCLC cell lines. ZFR mRNA level was determined by means of quantitative real-time PCR and normalized to the level of GAPDH mRNA. The fold changes of mRNA expression of indicated genes were compared as a ratio to the LO2. The data are shown as mean ± SD of triplicates experiments. $^{*}P < 0.05$, $^{**}P < 0.01$ compared with the LO2.

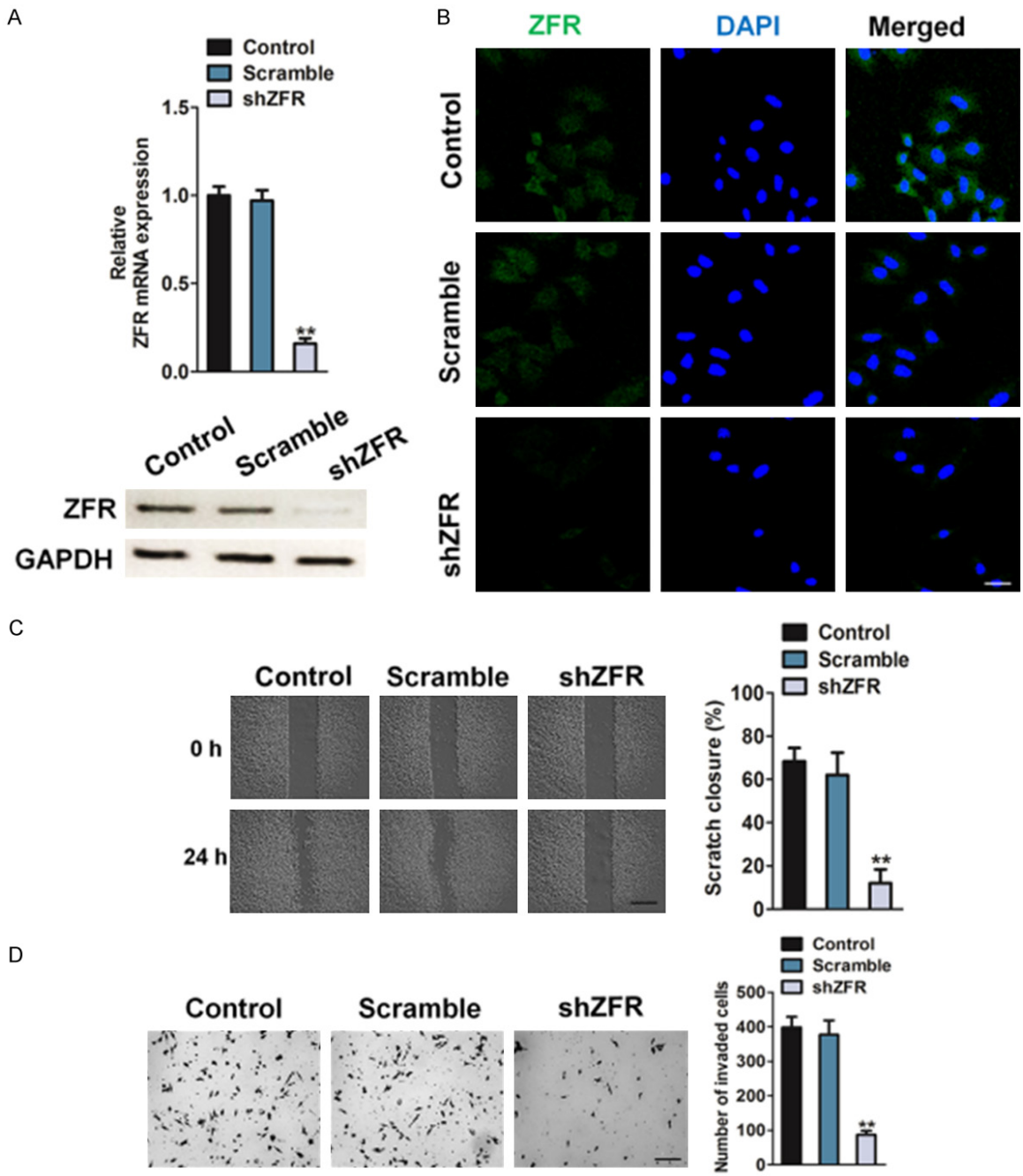

Figure 3. The effect of shZFR on NSCLC cells metastasis. A. The levels of ZFR in H1975 parental cells and cells stably expressing scramble control or shZFR were examined by qRT-PCR (upper panel) and western blotting (lower panel), respectively. B. H1975 cells were transfected with ZFR shRNA or control scramble. After for 48 h post transfections, cells were fixed and incubated with primary antibodies against ZFR and then were immunostained with anti-rabbit FITC-conjugated secondary antibody and then stained with DAPI. The specimens were visualized and photographed using a fluorescence microscope (Scale bar represents 50 μm). C. H1975 cells were plated in 6 cm dishes. A wound healing assay was performed to determine the metastatic potential of cells and representative pictures of the wound distance were taken at 0 h and 24 h post scratching as indicated. Scale bar represents 200 μm. D. H1975 cells transfected with either control scratched or ZFR targeted shRNA were subjected to a Transwell invasion assay. The invasive cells were stained and quantified. Data was collected from three individual studies and were mean ± SD. values $^{**}P < 0.01$, compared to control cells. Scale bar represents 100 μm.

lls, we transferred H1975 cells with ZFR shRNA to stably establish the H1975-shZFR cell line with shRNA specific for ZFR (**Figure 3A** and **3B**). We next investigated whether decreased

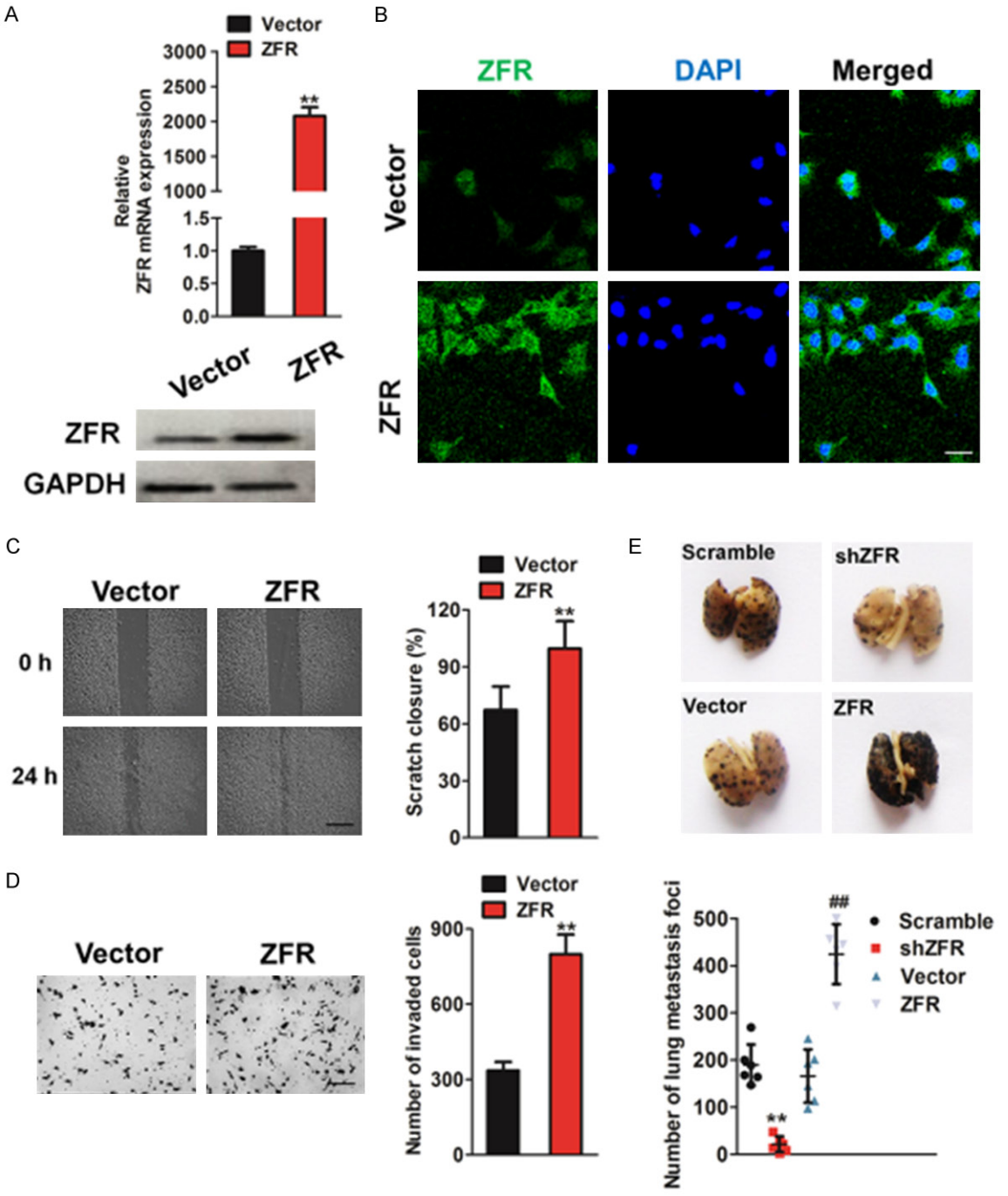

Figure 4. Confirmation of the Role of ZFR in NSCLC metastasis by overexpression. A. qRT-PCR analysis of ZFR expression in vector-control and ZFR-overexpressing H1975 cells (upper panel). The levels of ZFR protein in vector-control and ZFR-overexpressing H1975 cells were examined by western blotting (lower panel). B. Plasmid mediated ZFR protein overexpression was validated by immunofluorescence assay. Scale bar represents 50 μm. C. ZFR was cloned into vector and transfected into NSCLC H1975 cells. The cells transfected with an empty vector were used as control. The cell motility was determined by wound healing assay 24 h post scratching and the percentage of wound closure was quantified. Scale bar represents 200 μm. D. The cell invasion was evaluated by Transwell invasion assay. E. Representative images of lungs from mice were taken after 2 weeks of injection with B16F10 control cells, with shZFR or ZFR overexpressing B16F10 cells. Numbers of lung metastasis were quantified and showed by each point. $^{**}P < 0.01$, compared to control cells; $^{\#\#}P < 0.01$, compared to vector. Scale bar represents 100 μm.

H1975 cell metastasis could be imitated by gene silencing with shRNA specifically for ZFR.

In the wound healing assay, shZFR H1975 cells exhibited declined migration potency compared

to control cells. The control cells showed a markedly faster wound closure (**Figure 3C**). H1975-shZFR cells also displayed a significantly decelerated cell invasion profile in a Transwell invasion examination. As anticipated, ZFR silencing reduced the invasion (**Figure 3D**). Matrix metalloproteinases (MMPs) are a multi-gene group of zinc-based ECM-degrading endopeptidases involved in pathological phenomena such as carcinogenesis. Hence, we investigated the effect of ZFR knockdown on the activity of MMP-2/9. The activity of MMP-2/9 was remarkably reduced after a decrease of ZFR (Supplementary Figure 2). To confirm the biological role of ZFR up-regulation in NSCLC cell metastasis, H1975 cell lines that stably expressed ZFR were established (**Figure 4A** and **4B**). Ectopic expression of ZFR in H1975 cells dramatically increased metastasis, as evidenced by accelerated cell migration and invasion (**Figure 4C**, **4D**). Furthermore, overexpression of ZFR could also enhance the activity of MMP-2/9 (Supplementary Figure 3). Finally, to determine whether ZFR knockdown also results in an increase in tumor cells metastasis in vivo, the NSCLC cells B16F10 control, ZFR-OE (overexpression), or shZFR cells were injected intravenously into nude mice and lung metastasis was examined 12 weeks later. As shown in **Figure 4E**, there was a significant increase in the number of metastatic lesions produced by ZFR-OE cells compared to those produced by control cells. Conversely, transduction of B16-F10 cells with shZFR resulted in a reduction of the number of lung metastatic foci. Collectively, these results suggest that ZFR up-regulation promotes aggressiveness of NSCLC cells in vitro. These observations offer strong evidence for the role of ZFR in the promotion of metastatic potential in NSCLC.

The Notch1 pathway is involved in ZFR-mediated NSCLC cell metastasis

In order to unravel the cellular pathways involved in ZFR-mediated migration and invasion, we performed gene expression analysis in control and ZFR-depleted NSCLC cells. We selected a panel of 23 genes involved in the regulation of migration and invasion (**Figure 5A**). The most down-regulated gene was Notch1, which encodes the Notch1 protein, one of the canonical ligands for the Notch receptor family [22]. We confirmed that ZFR knockdown down-regulated both Notch1 mRNA and protein (**Figure 5B**). Notch1 regulates multiple cancer-associated processes including proliferation, survival, EMT, metastasis, and angiogenesis. We therefore evaluated the migration and invasion of H1975 cells after Notch1 depletion (Supplementary Figure 4). Notch1 knockdown significantly reduced both the migration and invasion potencies of H1975 cells (**Figure 5C**, **5D**). We then hypothesized that ZFR regulates NSCLC cell migration and invasion through Notch1 signaling. To confirm the role of Notch1 in ZFR-mediated NSCLC cell metastasis, a constitutively active form of Notch1 (pCLEN-Notch1) was introduced into ZFR-silenced cells. The expression of Notch1 was confirmed by Western Blot analysis using anti-Myc and anti-Notch1 antibodies (**Figure 6A**). Cell metastasis was then examined by wound healing and Transwell assays. As expected, active Notch1 largely restored the impaired migration and invasion of ZFR-silenced H1975 cells (**Figure 6B**, **6C**). These results identify Notch1 as a ZFR target that regulates NSCLC cell migration and invasion. Furthermore, FLI-06, a Notch1 inhibitor, was employed to determine the role of Notch1 signaling in cell migration. As shown in **Figure 6D**, over-expression of Notch1 mediated by ZFR was completely blocked by FLI-06. In addition, ZFR-promoted migration and invasion in H1975 cells was abolished by FLI-06, as shown by wound healing and Transwell assays (**Figure 6E**, **6F**). In conclusion, these data indicate that ZFR/Notch1 signaling is involved in metastasis of NSCLC cells.

NSCLC cell-intrinsic ZFR promotes tumor growth

We next examined whether NSCLC-specific ZFR shRNA or over-expression affects NSCLC cell growth in vitro, using an established culture system designed for the study of tumorigenic minority populations. ZFR shRNA impaired and ZFR-OE promoted cell proliferation in vitro compared to their respective controls (**Figure 7A**). Moreover, ZFR shRNA blocked and ZFR-OE promoted colony formation in vitro in comparison to their respective controls (**Figure 7B**). Because PI3K/AKT signaling in tumor cells modulates several downstream pathways, such as PI3K/AKT and mTOR signaling, which also serve critical roles in NSCLC-genesis, we next examined NSCLC ZFR-specific changes in phospho (p)-AKT, and p-S6 ribosomal protein levels. ZFR shRNA reduced and ZFR-OE increased phos-

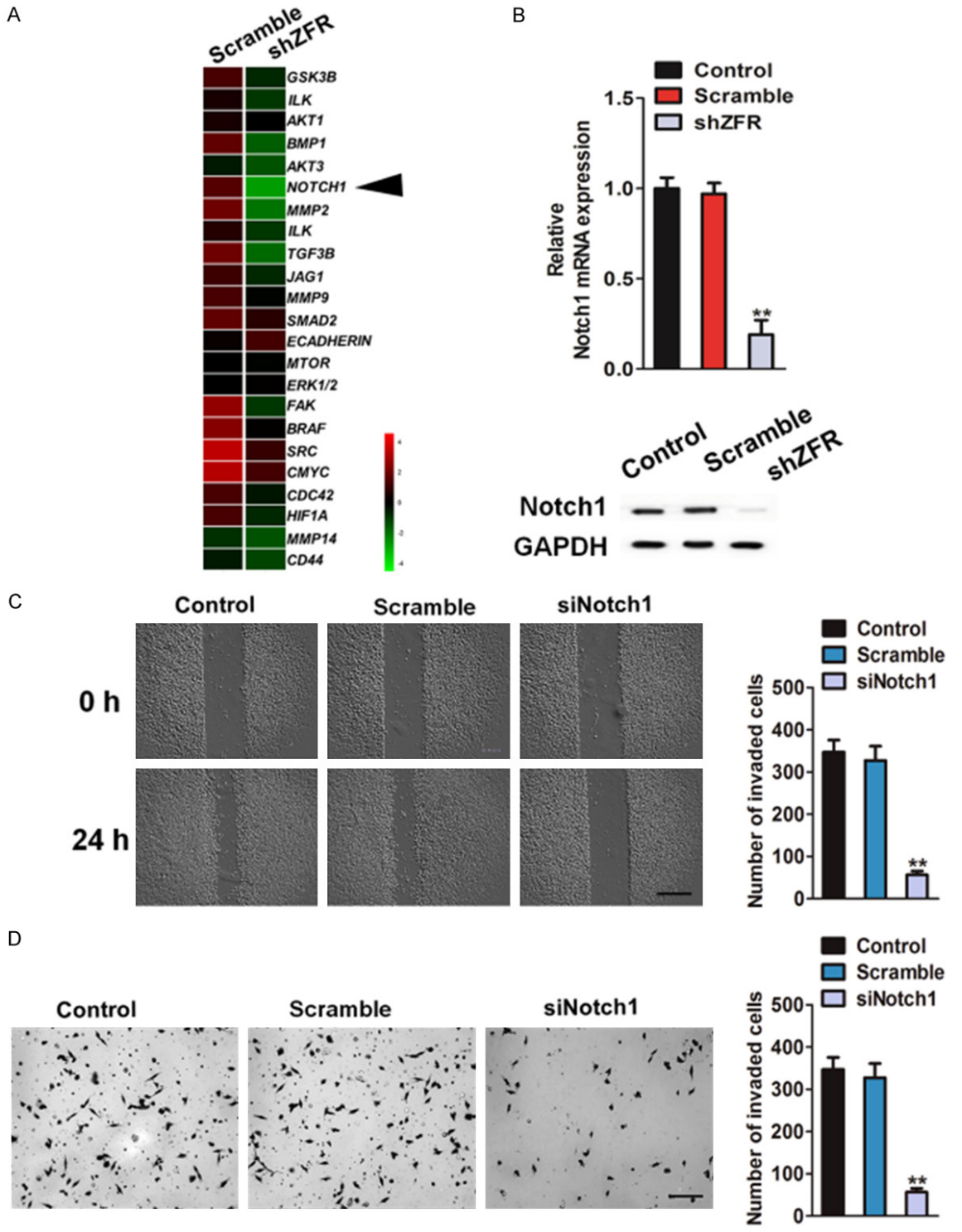

Figure 5. ZFR regulated Notch1 pathway in NSCLC cells. A. ZFR down-regulated the expression of pro-metastasis factors in shZFR cells. Gene expression analysis was executed by qRT-PCR contrasting control H1975 cells. Differentially modulated genes were selected and examined by hierarchical clustering. B. Notch1 mRNA (upper panel) and protein (low panel) expression were measured in H1975 cells 48 h after transfection with the indicated shRNA. C. Migration assay was conducted with scramble or siNotch1-depleted H1975 cells (right panel). Bars show means ± SD of three independent experiments. Data were from three independent experiments and were Mean ± SD. values. Scale bar represents 200 μm. D. Invasion assay was conducted with scrambled siRNA- or siNothc1-depleted H1975 cells. Bars show means ± SD of three independent experiments. Data were from three independent experiments and were Mean ± SD. values. The following symbols were used to indicate significant differences: $^{**}P < 0.01$. Scale bar represents 100 μm.

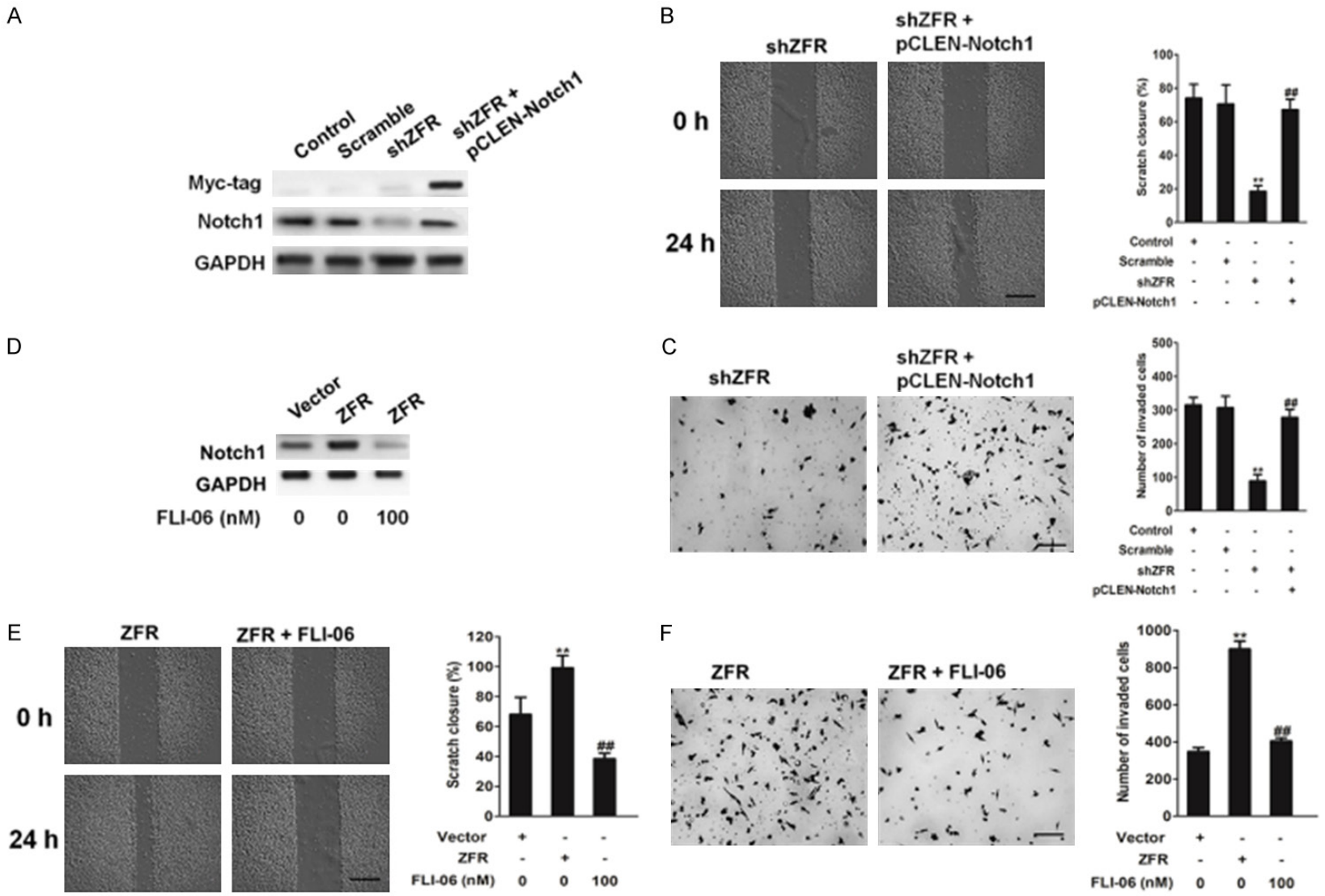

Figure 6. ZFR facilities the invasion and migration of NSCLC cells via Ntoch1 pathway. A. Expression of Notch1 was assessed by western blot with an antibody against Myc-tag and Notch1, and GAPDH was implemented as a loading control. B. Wound healing assay was executed to identify the cells motility co-transfected using ZFR silencing plasmid and pCLEN-Notch1 plasmid. Data were from three independent experiments and were Mean ± SD. values. $^{**}P < 0.01$ compared to control cells, $^{\#\#}P < 0.01$ compared to cells transfected with shZFR. Scale bar represents 200 μm. C. Invasion test was executed to identify the invasion of cells co-transfected with ZFR silencing plasmid and pCLEN-Notch1 plasmid. Data were from three independent experiments and were Mean ± SD. values. $^{**}P < 0.01$

compared to control cells, ##$P < 0.01$ compared to cells transfected with shZFR. Scale bar represents 100 μm. D. In the presence of FLI-06 (100 nM), cells were incubated for 1 h, protein extracts were analyzed by western blot with antibodies against Notch1. E. In the presence of FLI-06 (100 nM), wound healing assay was conducted to evaluate the cell motility after transfection. Data were from three independent experiments and were Mean ± SD. values. **$P < 0.01$ compared to cells transfected with vector, ##$P < 0.01$ compared to cells transfected with ZFR. Scale bar represents 200 μm. F. In the presence of FLI-06 (100 nM), Transwell invasion assay was conducted to evaluate the cell invasiveness after transfection. Data were from three independent experiments and were Mean ± SD. values. **$P < 0.01$ compared to cells transfected with vector, ##$P < 0.01$ compared to cells transfected with ZFR. Scale bar represents 100 μm.

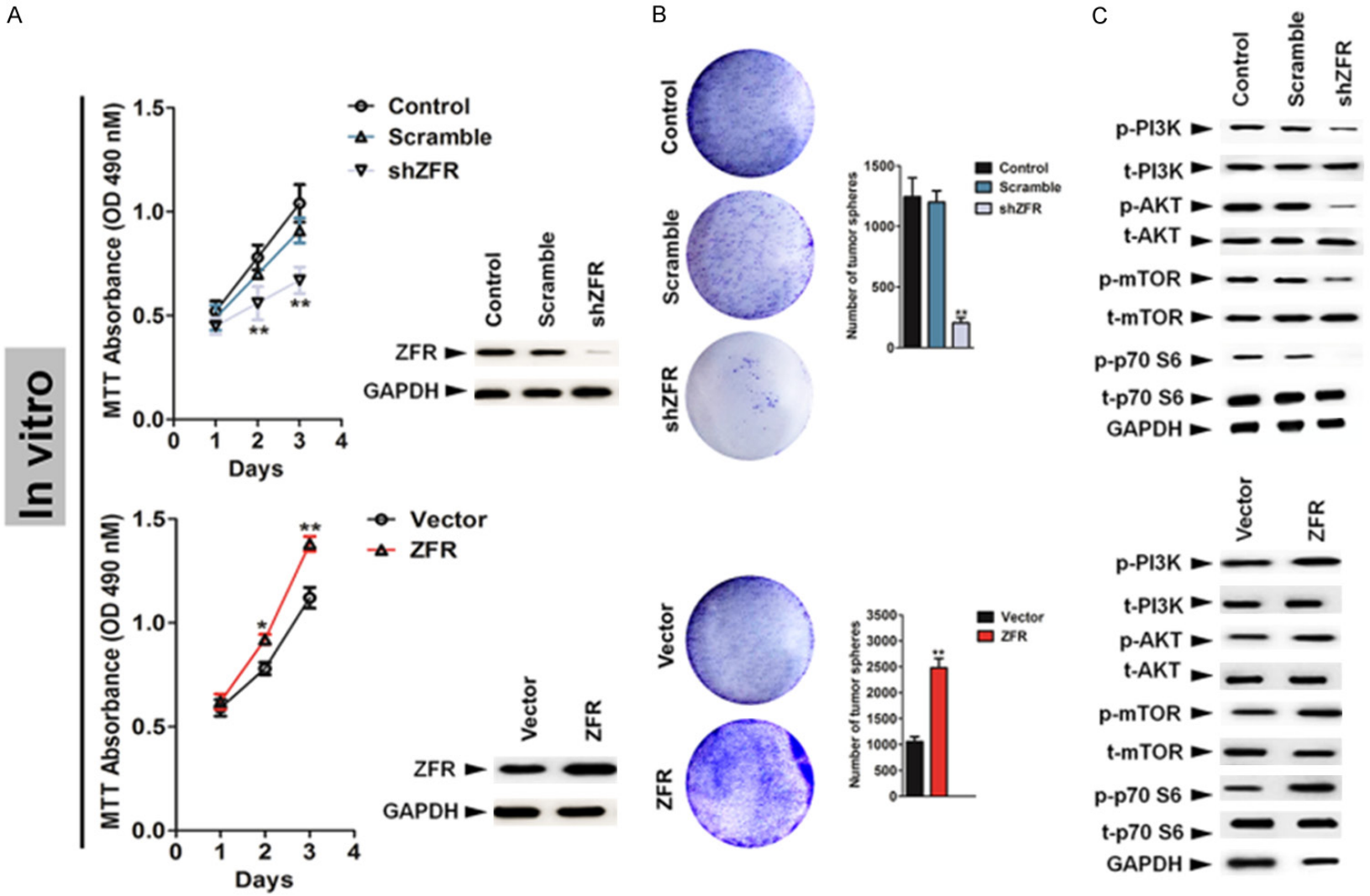

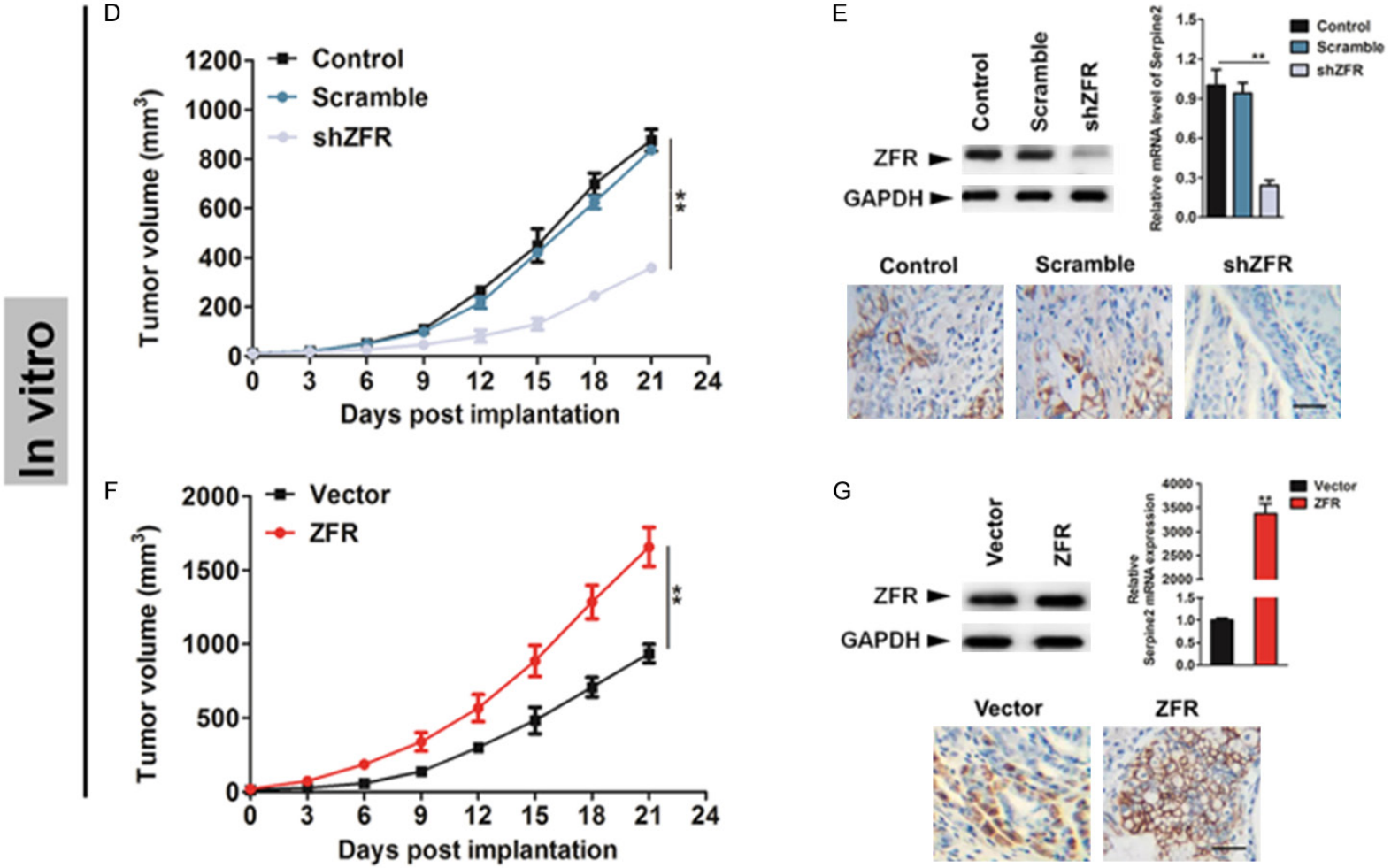

Figure 7. The effect of sHRNA ZFR on the tumor growth in vivo. A. MTT analysis of ZFR down-expression or over-expressing H1975 cells. B. Mean number of tumor spheres ± SD in ZFR-shRNA versus control (upper panel) and ZFR-OE versus vector-control H1975 NSCLC variants (low panel). Results were representative of three independent experiments. $^{**}P < 0.01$ compared to cells transfected with control cell. C. Immunoblot analysis of phosphorylated (p) and total PI3K, AKT, mTOR, and S6 in ZFR-shRNA versus control (upper panel) and ZFR-OE versus vector-control H1975 NSCLC variants (low panel). D. Tumor growth kinetics (mean ± SD) of ZFR-shRNA versus control H1975 NSCLCs in nude mice (n = 6 each). E. ZFR mRNA and protein expression (mean ± SD) determined by qRT-PCR and western blotting (upper panel). Representative immunohistochemical images of ZFR protein expression of H1975 NSCLCs harvested 21 days post inoculation of ZFR-shRNA versus control H1975 NSCLC cells to nude mice, respectively. Size bars, 50 μm. F. Tumor growth kinetics (mean ± SD) of ZFR-OE versus vector control H1975 NSCLCs in mice (n = 6 each). G. ZFR mRNA and protein expression (mean ± SD) determined by qRT-PCR and western blotting (upper panel). Representative immunohistochemical images of ZFR protein expression of H1975 NSCLCs harvested 21 days post inoculation o ZFR-OE- versus vector control-transduced H1975 NSCLC cells to nude mice, respectively. Size bars, 50 μm.

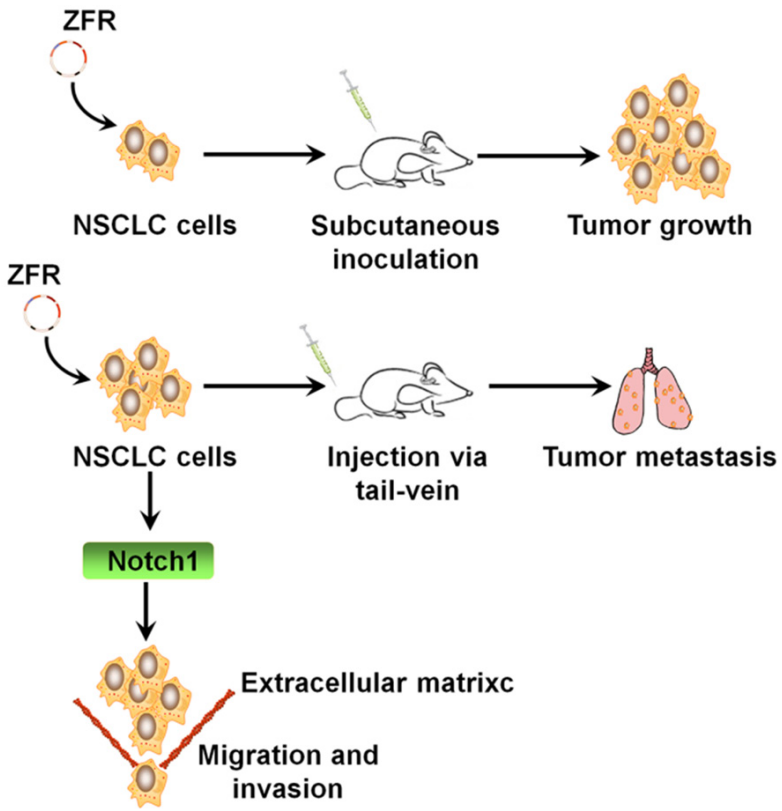

Figure 8. Proposed model by which ZFR promotes NSCLC growth and tumor metastasis.

phorylation of the mTOR effector molecule, S6, compared to that in control H1975 NSCLC cells (**Figure 7C**), indicating NSCLC-intrinsic, ZFR-mediated induction of protumorigenic mTOR pathway activity. To determine the potential role of NSCLC-expressed ZFR in experimental tumor growth, we next characterized ZFR expression in established NSCLC cell line growth in vitro and in vivo. ZFR shRNA and ZFR-OE H1975 NSCLC cells were inoculated subcutaneously into nude mice. Melanoma-specific ZFR shRNA and ZFR-OE resulted in decreased and increased H1975 NSCLC growth in nude mice, respectively, compared to that in the vector controls (**Figure 7D** and **7F**). ZFR shRNA NSCLC grafts demonstrated diminished ZFR mRNA and protein expression, while ZFR-OE NSCLCs exhibited significantly enhanced expression compared to that in control tumors at the experimental endpoint (**Figure 7E** and **7G**). Together, these in vitro findings suggest lymphocyte-independent, cancer cell-intrinsic functions of NSCLC-expressed ZFR in tumor growth.

Discussion

Malignant NSCLC is the skin cancer with the highest risk of death because of its highly metastatic potential [18]. Both incidence and mortality rate have continued to increase during the recent years. Tumor metastasis is a systematic procedure that uses complicated and optimally coordinated connections between a host microenvironment and tumor cells [19]. However, there is currently no effective treatment for metastatic NSCLC, in part because of the complicated mechanism underlying its metastasis. In the present study, we identified a novel role for ZFR in the metastasis of murine NSCLC cells. We found that ZFR promotes the metastasis of murine NSCLC cells in vitro and in vivo through the Notch1 signaling pathway. Our results may provide a new therapeutic target that could improve NSCLC treatment.

ZFR is becoming increasingly recognized as a key player in malignant cancers [20]. It was recently shown that human pancreatic cancer tumor cells with elevated ZFR metastasize more efficiently than control cells. ZFR overexpression plays an important role in malignant progression and metastasis in various cancer types [9]. In breast cancer, ECM proteomic analyses revealed up-regulation of ZFR in metastatic cancer cell lines and in tumor tissues. In addition, ZFR was up-regulated in numerous invasive tumors, including prostate, colorectal, breast, pancreatic, testicular, and oral squamous cancers. This plays a role in cancer progression and malicious expansion [21]. ZFR is up-regulated by ERK signal transduction and develops covalent complexes with its protease substrate in the ECM following secretion. Overall, these investigations unravel the complicated function of ZFR during tumorigenesis. Until now, no research described the role of ZFR in NSCLC metastasis. In the current study,

we found that ZFR is a novel player involved in the metastasis of NSCLC cells.

In this work, we first reported a novel role for ZFR in the metastasis of NSCLC cells. We found that the metastasis of H1975 murine NSCLC cells was significantly inhibited when ZFR was disrupted by insertional mutagenesis. Further investigations showed that gene silencing of ZFR significantly decreased metastasis of NSCLC cells, as revealed by wound healing and migration assays, and that this effect is specific to skin cancer cells. In contrast, the overexpression of ZFR in H1975 NSCLC cells greatly enhanced the migration of these cells. Most convincingly, ZFR silencing markedly impaired lung metastasis of murine NSCLC B16F10 cells in vivo. The underlying molecular mechanism for ZFR-regulated NSCLC metastasis was identified as being associated to the Notch1 signaling pathway. Our results showed that overexpression of ZFR in H1975 murine NSCLC cells induced up-regulation of Notch1 levels, and ZFR silencing led to reduced Notch1 expression. Furthermore, restoration of Notch1 expression by an active form of Notch1 could rescue the impaired migration of H1975 cells induced by ZFR silencing. In the presence of FLI-06, a specific inhibitor of the Notch signaling pathway, cell migration and invasion promoted by ZFR over-expression were significantly inhibited, as revealed by the Transwell migration and invasion assay. Owing to its important role in the metastasis of NSCLC H1975 cells, ZFR may serve as an attractive target for cancer therapy. In future studies, it would be worthwhile to elucidate the precise role of ZFR in the regulation of Notch1 signaling that mediates metastasis in NSCLC cells (**Figure 8**).

Disclosure of conflict of interest

None.

Address correspondence to: Dr. Ri Chen, Department of Cardiothoracic Surgery, Xiangya Hospital of Central South University, 87# Xiangya Road, Changsha 410008, Hunan, China. E-mail: chenricr@outlook.com

References

[1] Zhu Z, Yu T and Chai Y. Multiple primary lung cancer displaying different EGFR and PTEN molecular profiles. Oncotarget 2016; 7: 81969-81971.

[2] Tomida S, Koshikawa K, Yatabe Y, Harano T, Ogura N, Mitsudomi T, Some M, Yanagisawa K, Takahashi T, Osada H and Takahashi T. Gene expression-based, individualized outcome prediction for surgically treated lung cancer patients. Oncogene 2004; 23: 5360-5370.

[3] Chang H, Oh J, Zhang X, Kim YJ, Lee JH, Lee CT, Chung JH and Lee JS. EGFR protein expression using a specific intracellular domain antibody and PTEN and clinical outcomes in squamous cell lung cancer patients with EGFR-tyrosine kinase inhibitor therapy. Onco Targets Ther 2016; 9: 5153-5162.

[4] Wang X, Li M, Hu M, Wei P and Zhu W. BAMBI overexpression together with beta-sitosterol ameliorates NSCLC via inhibiting autophagy and inactivating TGF-beta/Smad2/3 pathway. Oncol Rep 2017; 37: 3046-3054.

[5] Wang D, Shi W, Tang Y, Liu Y, He K, Hu Y, Li J, Yang Y and Song J. Prefoldin 1 promotes EMT and lung cancer progression by suppressing cyclin A expression. Oncogene 2017; 36: 885-898.

[6] Renaud S, Seitlinger J, Falcoz PE, Schaeffer M, Voegeli AC, Legrain M, Beau-Faller M and Massard G. Specific KRAS amino acid substitutions and EGFR mutations predict site-specific recurrence and metastasis following non-small-cell lung cancer surgery. Br J Cancer 2016; 115: 346-353.

[7] Wang L, Shi Y, Ju P, Liu R, Yeo SP, Xia Y, Owlanj H and Feng Z. Silencing of diphthamide synthesis 3 (Dph3) reduces metastasis of murine melanoma. PLoS One 2012; 7: e49988.

[8] Zhao X, Chen M and Tan J. Knockdown of ZFR suppresses cell proliferation and invasion of human pancreatic cancer. Biol Res 2016; 49: 26.

[9] Meagher MJ, Schumacher JM, Lee K, Holdcraft RW, Edelhoff S, Disteche C and Braun RE. Identification of ZFR, an ancient and highly conserved murine chromosome-associated zinc finger protein. Gene 1999; 228: 197-211.

[10] Wei W, Tang C, Zhan X, Yi H, Li C. [Effect of DJ-1 siRNA on biological behavior of human lung squamous carcinoma SK-MES-1 cells]. Zhong Nan Da Xue Xue Bao Yi Xue Ban 2013; 38: 7-13.

[11] Krusche B, Ottone C, Clements MP, Johnstone ER, Goetsch K, Lieven H, Mota SG, Singh P, Khadayate S, Ashraf A, Davies T, Pollard SM, De Paola V, Roncaroli F, Martinez-Torrecuadrada J, Bertone P and Parrinello S. EphrinB2 drives perivascular invasion and proliferation of glioblastoma stem-like cells. Elife 2016; 5.

[12] Zhang W, Shi X, Peng Y, Wu M, Zhang P, Xie R, Wu Y, Yan Q, Liu S and Wang J. HIF-1alpha promotes epithelial-mesenchymal transition and metastasis through direct regulation of ZEB1

in colorectal cancer. PLoS One 2015; 10: e0129603.
[13] Xiao Y, Jiang Y, Song H, Liang T, Li Y, Yan D, Fu Q and Li Z. RNF7 knockdown inhibits prostate cancer tumorigenesis by inactivation of ERK1/2 pathway. Sci Rep 2017; 7: 43683.
[14] Qin Y, Tang B, Hu CJ, Xiao YF, Xie R, Yong X, Wu YY, Dong H and Yang SM. An hTERT/ZEB1 complex directly regulates E-cadherin to promote epithelial-to-mesenchymal transition (EMT) in colorectal cancer. Oncotarget 2016; 7: 351-361.
[15] Tsuchiya S, Fujiwara T, Sato F, Shimada Y, Tanaka E, Sakai Y, Shimizu K and Tsujimoto G. MicroRNA-210 regulates cancer cell proliferation through targeting fibroblast growth factor receptor-like 1 (FGFRL1). J Biol Chem 2011; 286: 420-428.
[16] Geng L, Chaudhuri A, Talmon G, Wisecarver JL, Are C, Brattain M and Wang J. MicroRNA-192 suppresses liver metastasis of colon cancer. Oncogene 2014; 33: 5332-5340.
[17] Sharpe DJ, Orr KS, Moran M, White SJ, McQuaid S, Lappin TR, Thompson A and James JA. POU2F1 activity regulates HOXD10 and HOXD11 promoting a proliferative and invasive phenotype in head and neck cancer. Oncotarget 2014; 5: 8803-8815.
[18] Tang Q, Zhao H, Yang B, Li L, Shi Q, Jiang C and Liu H. WIF-1 gene inhibition and Wnt signal transduction pathway activation in NSCLC tumorigenesis. Oncol Lett 2017; 13: 1183-1188.
[19] Taverna S, Pucci M, Giallombardo M, Di Bella MA, Santarpia M, Reclusa P, Gil-Bazo I, Rolfo C and Alessandro R. Amphiregulin contained in NSCLC-exosomes induces osteoclast differentiation through the activation of EGFR pathway. Sci Rep 2017; 7: 3170.
[20] Al-Souhibani N, Al-Ahmadi W, Hesketh JE, Blackshear PJ and Khabar KS. The RNA-binding zinc-finger protein tristetraprolin regulates AU-rich mRNAs involved in breast cancer-related processes. Oncogene 2010; 29: 4205-4215.
[21] Michalek JL, Lee SJ and Michel SL. Cadmium coordination to the zinc binding domains of the non-classical zinc finger protein Tristetraprolin affects RNA binding selectivity. J Inorg Biochem 2012; 112: 32-38.
[22] Jiang X, Zhou JH, Deng ZH, Qu XH, Jiang HY, Liu Y. [Expression and significance of Notch1, Jagged1 and VEGF in human non-small cell lung cancer]. Zhong Nan Da Xue Xue Bao Yi Xue Ban 2007; 32: 1031-1036.

Supplementary materials

Quantitative real-time PCR

Total RNA (0.5 μg) was isolated from cultured cells using TRIzol reagent (Invitrogen, USA). First-strand cDNA was synthesized with 1 μg total RNA using a PrimeScript RT reagent kit (TakaraBio, Japan). Quantitative real-time PCR was performed using iQ™ SYBR® Green Supermix and the iQ5 real-time detection system (Bio-Rad Laboratories, CA). The comparative cycle threshold (Ct) method was applied to quantify the expression levels through calculating the $2(-\Delta\Delta Ct)$ method. The primer pairs used for PCR were as follows (sense and antisense, respectively): GAPDH (forward, 5'-GGAGCGAGATCCCTCCAAAAT-3'; reverse, 5'-GGCTGTTGTCATACTTCTCATGG-3') was used as an internal control; ZFR (forward, 5'-TGGTGATGAGATACGGCGTAA-3'; reverse, 5'-GTTAGCCACTGTCACAATGTCTT-3'). cDNAs amplification and relative expression values were obtained from three independent experiments.

MMP-2/9 activity assay

The activity of MMP-2/9 was determined by QuickZyme Mouse MMP-2/9 activity assay (QucikZymeBioSciences, Netherlands) according to the manufacturer's instructions. Briefly, after transfection for 48 h, cells were washed with fresh medium and replaced with serum-free medium. After additional 24 h, the medium was collected and centrifuged at 10,000 g for 10 min. Respective supernatant was added to the 96-well strip coated with MMP-2/9 antibody and incubated at 4°C overnight. After washing with wash buffer for 4 times, 50 μl assay buffer was added into the well, followed by adding 50 μl detection reagent. After incubation at 37°C for 1 h, OD405 was measured with Tecan (Männedorf, Switzerland).

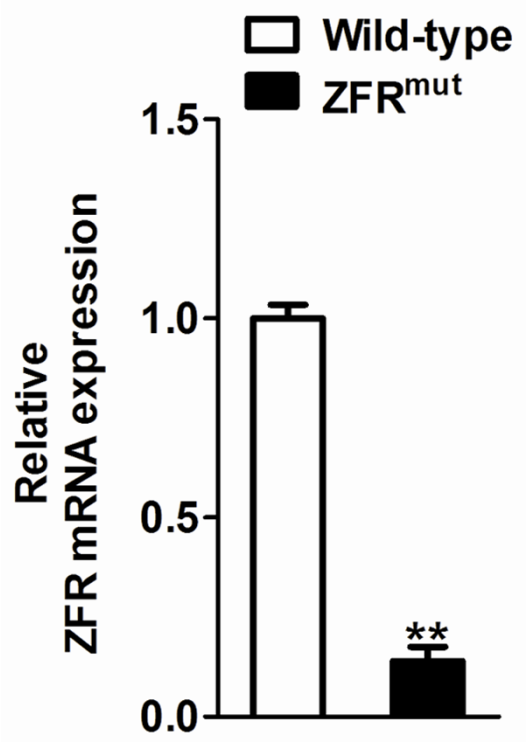

Supplementary Figure 1. qRT-PCR was performed to evaluate the mRNA level of ZFR in indicated H1975 cells. Histograms reporting the levels of ZFR mRNA (normalized to the GAPDH mRNA) as assessed in indicated cancer cell lines. Mean ± SD of three independent experiments. For indicated comparisons, $^{**}P < 0.01$.

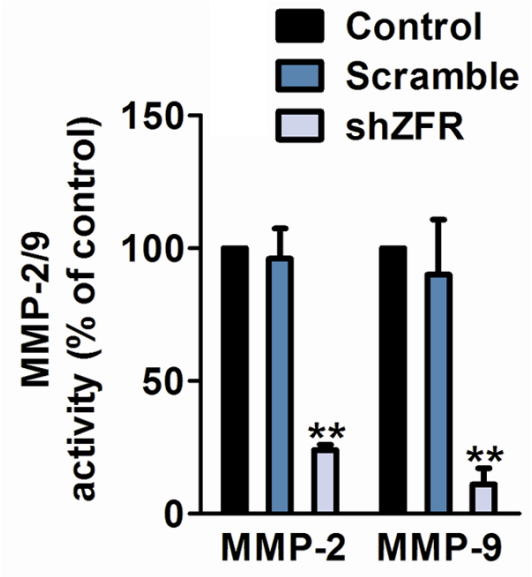

Supplementary Figure 2. H1975 cells were transfected with either control scramble or ZFR targeted shRNA. Activity of MMP-2/9 in indicated cells was determined by MMP-2/9 activity assay. Data are from three independent experiments and are average ± SD. values. $^{**}P < 0.01$, compared to control cells.

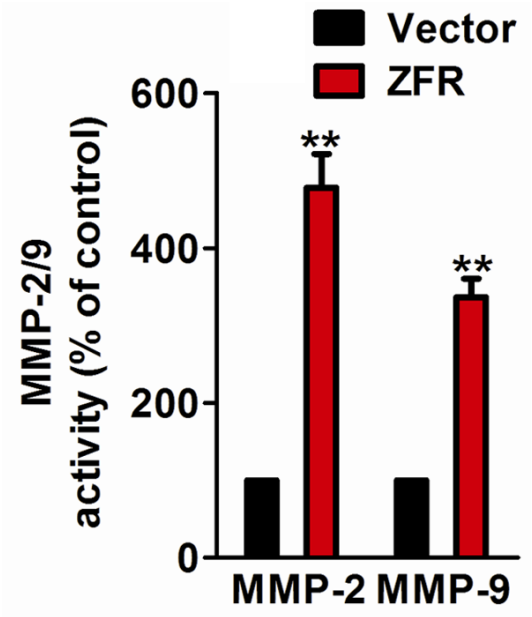

Supplementary Figure 3. ZFR was cloned into vector and transfected into H1975 cells. Activity of MMP-2/9 in control and ZFR-overexpression cells was determined by MMP-2/9 activity assay. Data are from three independent experiments and are average ± SD. values. $^{**}P < 0.01$, compared to control cells.

Supplementary Figure 4. Immunoblot validates Notch1 depletion in H1975 48 h after transfection with the indicated siRNAs.